STUDIA INFORMATICA 2009
Volume 30 Number 4 (87)

Andrzej ZACHER
Politechnika Śląska, Instytut Informatyki

MATHEMATICAL MODEL OF HUMAN TISSUE IN PHOTODYNAMIC CANCER RECOGNITION[1]

Summary. This paper presents the method of light propagation in human tissue. Subsurface scattering model together with photon mapping is applied to generate images. Surface and volumetric photon maps were used to fully describe the fluorescence phenomenon. The qualitative comparison between images will be presented to find the best camera angle of incidence. Moreover, multi-spectral images rendered during simulations are verified with real, scientific images.

Keywords: photodynamic diagnosis, light transport simulation, subsurface scattering, fluorescence model, photon mapping, endoscopy

MATEMATYCZNY MODEL TKANKI LUDZKIEJ W FOTODYNAMICZNEJ DIAGNOZIE I ROZPOZNAWANIU RAKA

Streszczenie. Artykuł przedstawia zastosowanie metody propagacji światła w stosunku do tkanek ludzkich. Model podpowierzchniowego rozpraszania razem z algorytmem mapowania fotonów zostały użyte do generowania obrazów. Aby w pełni symulować zjawisko fluorescencji, wykorzystano powierzchniowe i wolumetryczne mapy fotonów. Została przeprowadzona analiza jakościowa otrzymanych obrazów, w zależności od kąta nachylenia endoskopu. Ponadto, multispektralne obrazy wygenerowane w czasie eksperymentów, zweryfikowano z rzeczywistymi zdjęciami.

Słowa kluczowe: diagnoza fotodynamiczna, symulacja transportu światła, rozpraszanie podpowierzchniowe, model fluorescencji, mapowanie fotonów, endoskopia

[1] Supported by Ministry of Science and Higher Education grant R13 046 02

1. Introduction

Global illumination in scenes can be simulated with general bidirectional scattering distribution functions (BSDF). They contain illumination information in form of photons which are distributed by light rays. Stored in photon maps can be later used for the image generation with view paths traced from the camera [1].

The photon map algorithm has some desirable properties that makes it useful in global illumination computations. It is relatively fast and simple to parallelize. It can handle a mixture of specular, glossy, and diffuse reflection and transmission including caustics effect. It can handle very complex scenes, since the photon map is independent of surface representation [2].

In order to describe the model of light transport in human tissue, some additional computations need to be performed besides normal Photon Mapping. Reflection of a photon at air-tissue or tissue-tissue boundaries must be calculated. Once entered the tissue, the photon is moved a given distance where it may be absorbed, scattered, reflected internally or out of the tissue. Then new scattering angle is generated and the photon is repetitively moved until it either is completely absorbed or escapes from the tissue. If the photon is absorbed, the position of that incident is recorded. If the photon escapes from the tissue, the transmission or reflection of the photon is stored. This procedure is repeated until the desired number of photons have been traced and recorded. As the number of photons propagated approaches infinity, the overall reflection, transmission, and absorption profiles approach real values. This data can be later compared with medical investigations for the tissue with similar optical properties [3].

The model of a human tissue with its morphological properties was introduced in [4] and in this paper it is going to be only shortly described. Moreover, in vivo and ex vivo studies presented in [5], give some details about fluorescence from endogenous and exogenous molecules in cells and tissues.

2. Previous work

Monte Carlo model of steady-state light transport in multi-layered tissue was presented in [4]. It describes local rules of photon propagation. When a scattering event occurs the angles of deflection in a photon's trajectory and the step size of photon movement during photon-tissue interaction depend on probability distribution functions. Because this method is strictly statistical and requires a large amount of computation time. Moreover, the simple model of

tissue was introduced, but fluorescent properties were missing. Also phase and polarization were not implemented, but still it could be used to simulate light transport correctly.

In [6], Bidirectional Surface Scattering Reflection Distribution Function was introduced. A dipole point source diffusion for single scattering event was considered as the extension of common BRDF model. The idea was based on the assumption, that light that leaves a material at different position than it initially entered. Despite of the fact, that all those changes can be applied rather easily, the algorithm does not allow the photons to get under the surface of the material where the fluorescent phenomenon occurs. It is basing on the surface photon map.

The idea of photon map was additionally extended in [7]. In order to reduce noise and increase efficiency, volumetric photon map containing photons stored in participating media was generated. New radiance estimate together with surface photon mapping enable to render multiple volume scattering in translucent media.

In [8] the optical effects of translucency and coloration due to the composition of minerals near the surface was demonstrated for granite, marble and sandstone models of statues. Again, the simulation of the scattering of light inside the stone was performed using a general subsurface Monte Carlo ray tracer.

Volume photon mapping that includes fluorescence phenomenon was presented in [9]. They solved the Full Radiative Transfer Equation (FRTE) and apply Fermat's law, to simulate a global illumination solution which supports non-linear light paths. Physically-correct simulation of volume fluorescence in participating media, caused by inelastic scattering, including efficient computation of caustics was introduced.

Volumetric photon mapping was also used to simulate light propagation in smoke [10] and multi-scattering in human hairs [11]. Some optimization methods were presented in [12].

Although the light propagation in human tissue is rather good known topic described in literature, the qualitative analysis of its properties and influence of incident angle on the final appearance of image and cancer recognition was not done. Simulations in this is paper are going to show how images from different view angle looks like and suggest which one is the best. Also, a comparison between obtained results and real images is going to be performed.

3. Internal properties of human tissue

The human tissue is defined as infinitely long and wide single-layered structure with thickness long enough to absorb all the light. The key parameters are the following:

- refractive index n_{layer}=1.1,
- absorption coefficient u_a=20cm^{-1} (the probability of photon being absorbed per unit infinitesimal pathlength),
- scattering coefficient u_s=200cm^{-1} (the probability of photon being scattered per unit infinitesimal pathlength),
- anisotropy factor g=0.9 (the average of cosine value of deflection angle).

The top ambient medium was air with refractive index equal to 1. This model was widely described in [4] and proved by laboratory investigations.

Despite of the fact that light is absorbed and scattered under the surface of the object, its spectrum also changes relatively to material the tissue consists of. It was assumed that collagen and protoporphyrin molecules are dominant fluorophores that influence the color of light rays. To model the fluorescence phenomenon additional parameters were intrduced:

- the probability of interaction a photon sample with a fluorophores defined as $d_{collagen}$=0.2 and $d_{protoporphyrin}$=0.1,
- the concentration of fluorescent molecules in fluorophore described as $c_{collagen}$=0.4 and $c_{protoporphyrin}$=0.33.

Finally, Excitation-emission matrix (EEM) that uniquely identifies each fluorophore during interaction with photon was included. It describes how the emission spectra changes for different light excitation spectrum [13].

4. Storing photons

Photon mapping is an approach for solving the Light Transport Equation based on biased algorithm. It tries to separate the representation of a scene from its geometry and collects illumination information in a special data structure i.e. balanced the kd-tree. Each node contains the data about the coordinates of the hit point, color spectrum and incident direction of the photon. If the photon interacted with structure on the air-tissue boundary, then the packet is stored in surface photon map. Otherwise the photon is recorded in the volumetric photon map, that is related to the whole volume of the tissue.

Photon mapping can be divided into two separate parts. In the first step, packets of energy, represented by a light spectrum, are initiated and traced into the scene using Halton sequence. When a photon hits a tissue, Snell's law determines if the packet is reflected back or enters the tissue. In both cases, photon's weight needs to be decreased.

If the packet entered the tissue, then in every iteration its position is changed and energy gets attenuated. However, the photon is not only absorbed. Its spectrum can change as well depending on the type of interaction the packet undergoes. If one of the fluorophores, the

human tissue consists of, was hit by a photon, then the spectrum of the photon is updated using EEM. Finally photon's properties like spectrum, together with its position and direction are stored in volumetric photon map. This packet of energy is identified as fluorescent and in every iteration it is going to be stored in the photon map. In the second pass of photon mapping algorithm, data from the surface and volumetric photon maps are used to render images.

Just after the weight of the photon was updated, the packet is ready to be moved in the new scattering direction computed utilizing Heney-Greenstein phase function. This process of moving and updating a packet is finished, if either the weight of the photon is too small – verified by Russian Roulette – or the photon escapes the tissue. If this is a case for a fluorescent photon, then it is stored in the surface photon map [4].

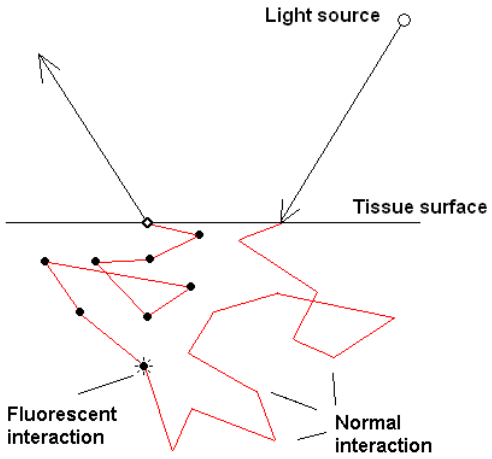

Fig. 1. Photons interact many times with molecules changing their direction. Only some fraction of them escapes the tissue and is stored into surface photon map (open dot). Others are completely absorbed. If the fluorescence phenomenon occurs, what happens very rarely, the photon is stored into volumetric photon map every time it interacts with tissue (closed dots)

Rys. 1. Fotony oddziaływają z tkanką bardzo często, co powoduje zmianę ich kierunku. Tylko niewielka ich część wyjdzie na powierzchnię i zostanie zapisana w powierzchniowej mapie fotonowej (oznaczono okręgami). Reszta fotonów jest całkowicie wchłonięta. Jeśli zajdzie zjawisko fluorescencji, co zdarza się bardzo rzadko, to od tego momentu foton ten będzie dopisywany do wolumetrycznej mapy fotonów przy każdej interakcji z tkanką (oznaczono kropkami)

5. Ray marching and rendering phase

In the second pass of the algorithm the scene is rendered using photon maps from the first pass. It means, that usual ray tracing process is performed by shooting rays from the camera. When a ray hits a given point on a surface, the radiance seen directly by the observer can be defined as:

$$L(x,\omega) \approx T_r(x \leftrightarrow x_S)L(x_S,\omega) + (\sum_{t=0}^{S} T_r(x \leftrightarrow x_S)\sigma_S(x_t)L_i(x_t,\omega)\Delta x) \quad (1)$$

where:

S – number of steps (in our simulations S=5),

$\sigma_S(x_t)$ – extinction coefficient equal to u_a+u_s (constant inside tissue),

$\tau(x \leftrightarrow x_S)$ – optical thickness defined as $\int_{x_S}^{x} \sigma(x)dx = x_S = x$,

$T_r(x \leftrightarrow x_s)$ – transmittance defined as $e^{-\tau(x \leftrightarrow x_S)}$,

$L(x_S, \omega)$ – direct illumination computed from ray tracing,

$L_i(x_t, \omega)$ – in-scattered radiance computed using photon maps,

Δx – length of each segment (constant for every t).

The final radiance at the point is the sum of the incident illumination and the sum of in-scattered radiances along the ray inside tissue. This idea is called Ray Marching, when at each step the contribution of photons is calculated and summed up. The first point on that ray (for t=0) is located on the surface level and computed using surface photon map. Illumination of all other points is defined by volumetric photon map [12]. Moreover, for surface photon map neighbor photons are gathered from the disc around query point. For volumetric map, a sphere around point of interest is searched for the nearest photons. In other words:

- for surface photon map

$$L_i(x_t,\omega) \approx \sum_{i=1}^{n} \frac{p(x_t,\omega,\omega_i)\Delta\Phi_i}{\pi r^2} \quad (2)$$

- for volumetric photon map

$$L_i(x_t,\omega) \approx \sum_{i=1}^{n} \frac{p(x_t,\omega,\omega_i)\Delta\Phi_i}{\frac{4}{3}\pi r^3} \quad (3)$$

where:

$p(x_t, \omega, \omega_i)$ – normalized phase function,

$\Delta\Phi_i$ – the power of photon i,

r – max. radius where neighbor photons were found,

n – number of neighbor photons.

However, the illumination at the point is not the same in all directions. It was assumed that the tissue surface is not Lambertian surface and radiance is angle dependent. It was accomplished by adding a small specular component described by simple Gauss function to reflection formula.

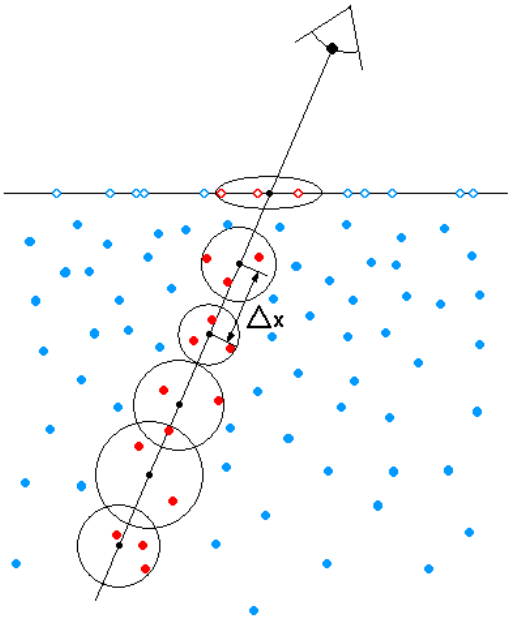

Fig. 2. Ray marching and photon gathering with constant step size. Open dots represent photons in surface photon map, closed dot symbolize photons in volumetric photon map

Rys. 2. Iteracja wzdłuż promienia ze stałym krokiem i gromadzenie fotonów. Okręgi reprezentują fotony w powierzchniowej mapie fotonów, natomiast kropki symbolizują fotony w wolumetrycznej mapie fotonów

6. Simulation and results

PBRT is a non-commercial computer program, which functionality was extended by the implementation of full Monte Carlo model of light transport in turbid media i.e. subsurface photon mapping algorithm. This software was written in C++ and is available with source code and book [14]. However, in order to make it easy to understand PBRT is poorly optimized. The time, needed to simulate subsurface scattering in tissue using photon mapping, was in range between 1-2 hours depending on the scene configuration.

The simulation was performed on the enhanced tissue model. Cancerous changes, where protoporphyrin was concentrated (red color), give the most interesting information for medicine. They want to identify such situations as quick as possible. The rest of structure contains collagen only (blue color).

Camera and lights are located on the head of the real endoscope, that is normally used during medical diagnosis. Fig. 4 and 5 describe the approximate model of a device with user-defined parameters. In the middle of the apparatus two light sources are located, described as area lights with cone angle α=45º. Moreover, angle β defines a rotation of the endoscope's head in relation to the tissue surface.

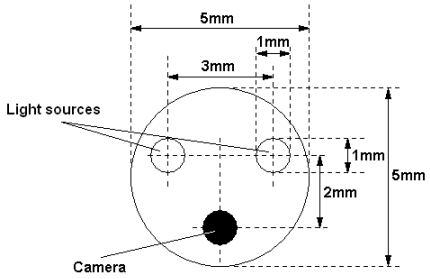

Fig. 3. Schema presenting the head of endoscope – bottom-view. Parameters are similar to the real device and were used during simulations
Rys. 3. Schemat głowicy endoskopu – widok z dołu. Parametry są zbliżone do rzeczywistego urządzenia i zostały wykorzystane w trakcie symulacji

For this tissue model six images were rendered for different angle of view β every time. In order to obtain good looking results, it was necessary to store 300000 photons in surface photon map and 300000 photons in volumetric photon map. Only photons which spectrum changed during interaction with fluorescent molecules were recorded and used in the process of rendering.

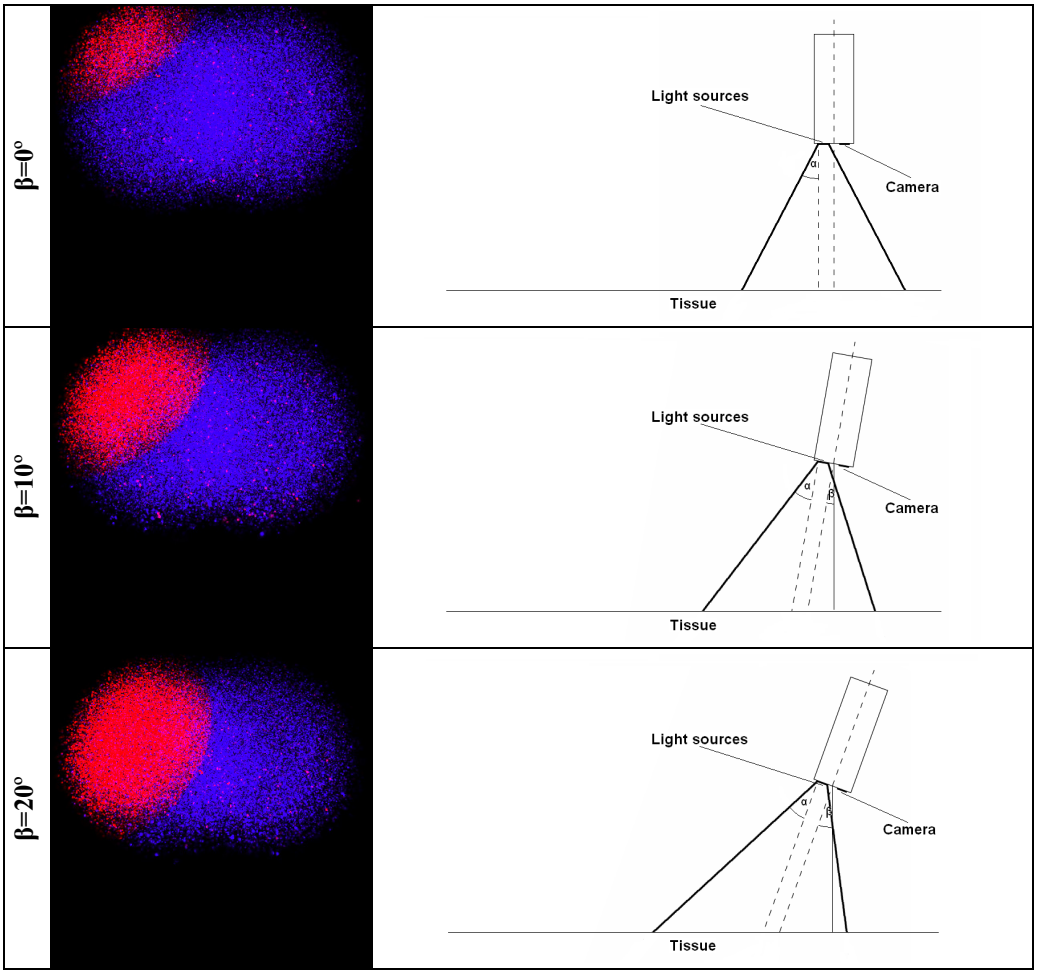

Fig. 4. Tissue surface for different camera angle of view β (0÷20º)
Rys. 4. Powierzchnia tkanki dla różnego kąta nachylenia kamery β (0÷20º)

Best quality images were obtained for β between 0º and 30º. For larger angles images get darker and darker, what is especially visible on light borders. It means that the number of photon traced in the scene should be changed for different views of camera. That value cannot remain constant, otherwise the image is not clear and smooth any more.

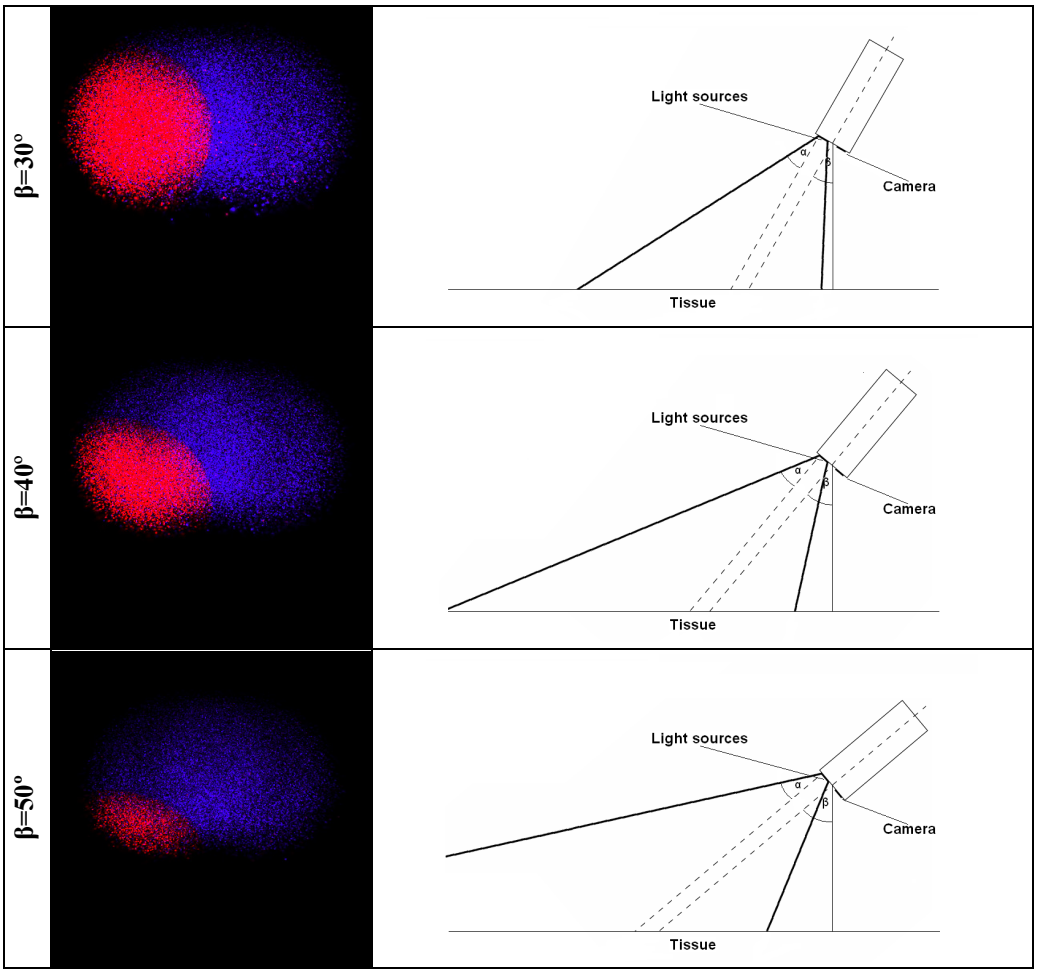

Fig. 5. Tissue surface for different camera angle of view β (30÷50º)
Rys. 5. Powierzchnia tkanki dla różnego kąta nachylenia kamery β (30÷50º)

Looking at red part of all pictures, where cancerous polyp was added and protoporphyrin concentrated, better results were obtained for angles 20º and 30º. Its appearance is rather uniform and that structure is stronger illuminated.

Quantitative analysis would give more accurate results, but even now it seems that the best angle of view is not 0º. Simulations point out that for the best angle β, one should look somewhere else, probably around 20÷30º interval. This is going to be the goal of other experiments.

7. Verification of tissue model

The Institute of Oncology in Bytom was asked to perform a special experiment. A droplet of endo-protoporphyrin IX – widely used photosensitizer in photodynamic diagnosis – was laid down onto the piece of material. A multi-spectral camera took images for wavelengths in range 400÷720 nm and constant step size 16 nm.

Those imaged were further compared with multi-spectral images of simplified tissue model. It assumes, that tissue consist of only one fluorophore. Unfortunately, the Emission-Excitation Matrix (EEM) for endo-protoporphyrin IX was not available, so it was only possible to use a fluorophore with very similar properties i.e. normal photoporphyrin. The results of comparison are presented in Fig. 6 and 7.

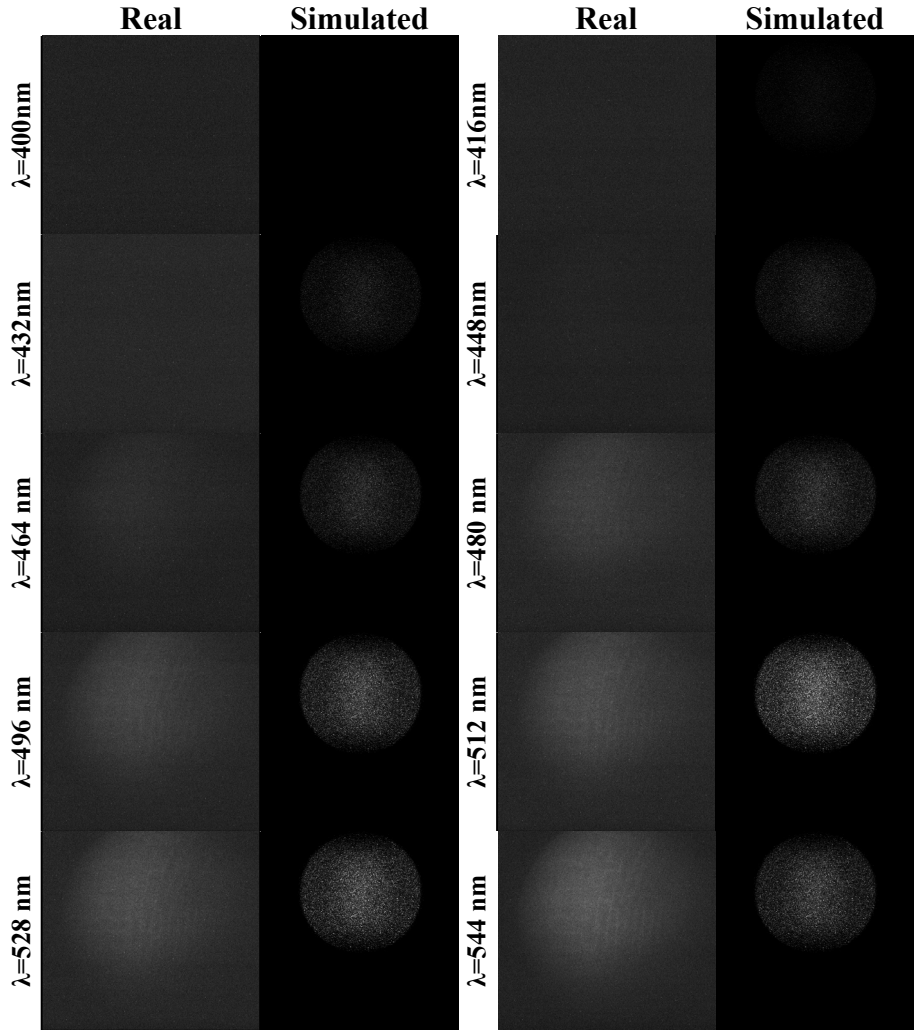

Fig. 6. The comparison of multi-spectral images of real protoporphyrin and simulated one for different wavelength λ (400÷544 nm)

Rys. 6. Porównanie multispektralnych obrazów rzeczywistej protoporfiryny i zasymulowanej dla różnych długości fali λ (400÷544 nm)

It is quite good visible that changes in real multi-spectral images are followed by the simulation. Despite of the fact that slight errors are visible for 432 nm and 448 nm images – where computer-generated pictures have some intensity, whereas originals are still black – presented model still behaves well. Moreover, in the end of range, the intensity of real images fades earlier than for simulated pictures, but again changes are perceived as similar.

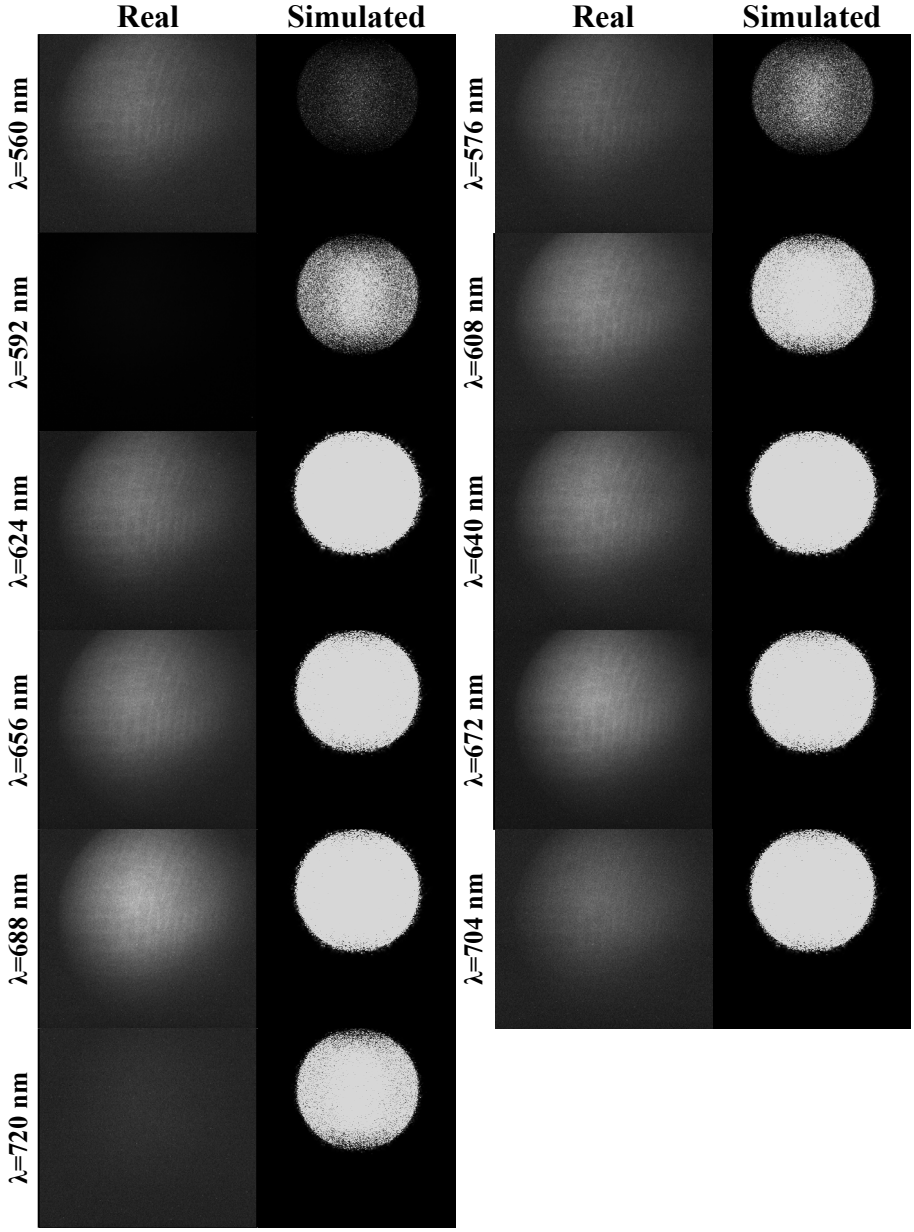

Fig. 7. The comparison of multi-spectral images of real protoporphyrin and simulated one for different wavelength λ (560÷720 nm)

Rys. 7. Porównanie multispektralnych obrazów rzeczywistej protoporfiryny i zasymulowanej dla różnych długości fali λ (560÷720 nm)

One of the reasons, that respective images look different for the same wavelength, is mismatch of characteristics between protoporphyrin and endo-protoporphyrin IX. The simulation could be performed again, if appropriate matrices were provided.

There is also one image for wavelength 592 nm that completely doesn't match the intensity profile of a droplet of protoporphyrin – it is totally black. This error should be not considered in further analysis, but it points out that the apparatus and spectroscopic devices were not ideal.

8. Discussion and future work

Images generated during simulations are not perfect and lack quality, that could be enhanced by increasing the number of photons. However, in such a case time needed to perform the simulation would be extended from one hour to many hours, what is not desired at this stage of work. Obtained pictures show that for big incident angles, the energy of photons get smaller and distances between them get longer. This effect creates areas of surface that are not covered by photons and consequently perceived as black by the observer. Images for β greater than 30º should be corrected, but their intensity remains unchanged anyway, because of tissue absorption.

Simulation of droplet of protoporphyrin was performed and compared with real multi-spectral images. It is interesting that obtained pictures quite good matches the originals. Besides of the fact that another EEM was used, this experiment gives promising result. A better verification of tissue model could be done, if multi-spectral images of authentic cancerous tissue were available. Basically, it is very difficult to obtain them, because images for different wavelength are taken separately. Even a tiny move of investigated tissue causes that pictures do not show the same part of the structure and cannot be compared with generated images. Anyway, this topic should be further investigated, because for ideal multi-spectral images, it could be possible to adjust the model and predict what substances the tissue is made of and simulate it better. That would be a milestone in implementation of perfect tissue simulation.

BIBLIOGRAPHY

1. Hey H., Purgathofer W.: Global illumination with photon map compensation. TR-186-2-01--04, January 2001.
2. Christensen P. H.: Faster photon map global illumination. Journal of Graphics Tools, 4(3):1.10. ACM 1999.

3. Prahl S. A., Keijzer M., Jacques S. L., Welch A. J.: A Monte Carlo model of light propagation in tissue, SPIE Proceedings of Dosimetry of Laser Radiation in Medicine and Biology, IS 5, 1989, p. 102÷111.
4. Wang L., Jacques S. L.: Monte Carlo modeling of light transport in multi-layered tissues in standard C. University of Texas M. D. Anderson Cancer Center, 1992.
5. Latos W., Kawczyk-Krupka A., Ledwon A., Kosciarz-Grzesiok A., Misiak A., Sieron-Stoltny K., Sieron A.: The role of autofluorescence colonoscopy in diagnosis and management of Solitary Rectal Ulcer Syndrome. SPIE Photonics West- Conferences and Courses. Biomedical Optics.Imaging, Manipulation and analysis of Biomolecules, Cells and Tissues VI. Cell and tissue functional imaging. San Jose 2008.
6. Jensen H. W., Marschner S. R., Levoy M., Hanrahan P.: A practical model for subsurface light transport. In Proceedings to Siggraph, 2001, p. 511÷518.
7. Jensen H. W., Christensen P. H.: Efficient simulation of light transport in scenes with participating media using photon maps. In Proceedings of SIGGRAPH'98, Orlando, July 1998, p. 311÷320.
8. Dorsey J., Edelman A., Jensen H. W., Legakis J., Pedersen H. K.: Modeling and rendering of weathered stone. In Proceedings of SIGGRAPH'99, August 1999, p. 225÷234.
9. Gutierrezy D., Munoz A., Anson O., Seron F. J.: Non-linear volume photon mapping. Eurographics Symposium on Rendering, 2005.
10. Zhou K., Ren Z., Lin S., Bao H., Guo B., Shum HY.: Real-time smoke rendering using compensated ray marching. International Conference on Computer Graphics and Interactive Techniques, ACM SIGGRAPH 2008.
11. Moon J. T., Marschner S. R.: Simulating multiple scattering in hair using a photon mapping approach. ACM Transactions on Graphics 25:3 Proceedings of SIGGRAPH 2006.
12. Jarosz W., Zwicker M., Jensen H. W.: The beam radiance estimate for volumetric photon mapping. Eurographics, Vol. 27, No. 2, Crete, April 2008.
13. Li BH., Xie SS.: Autofluorescence excitation-emission matrices for diagnosis of colonic cancer. World J Gastroenterol,11(25) , 2005, p. 3931÷3934.
14. Pharr M., Humphereys G.: Physically based rendering. From theory to implementation. Morgan Kaufmann, 2004.

Recenzent: Dr hab. inż. Maria Pietruszka, prof. Pol. Łódzkiej

Wpłynęło do Redakcji 14 lipca 2009 r.

Omówienie

Tkanki ludzkie mają tę specyficzną właściwość, że promienie światła nie tylko są odbijane od ich powierzchni, ale również wnikają do ich środka, gdzie są absorbowane lub ponownie rozpraszane. W końcu ich energia jest tak mała, że zostają kompletnie pochłonięte przez materiał albo, pomimo wielu interakcji z tkanką, z powrotem wracają na powierzchnię. Oprócz tego promień światła może wziąć udział w zjawisku fluorescencji, w wyniku którego jego widmo ulegnie zmianie.

Cały ten proces można stosunkowo łatwo opisać rozszerzonym algorytmem mapowania fotonów. Oprócz standardowej powierzchniowej mapy fotonów, tworzona jest także mapa wolumetryczna, gdzie przechowywane są wszystkie interakcje fotonu z tkanką. Głównym założeniem jest niekoncentrowanie się na zwykłych fotonach, ale tylko na tych, które uczestniczyły w procesie fluorescencji (rys. 1). Dzięki zastosowaniu dwóch map fotonowych możliwe jest policzenie radiancji na powierzchni tkanki jako (1). Sposób liczenia wpływu fotonów wolumetrycznych na iluminacje na powierzchni tkanki został przedstawiony na rys. 2.

W wyniku przeprowadzenia kilku symulacji dla różnych kątów padania promieni światła najbardziej wyraźny obraz części rakowej tkanki udało się uzyskać dla kątów 20÷30º (rys. 4 i 5). Bardziej dokładne różnice pokazałaby analiza ilościowa algorytmu. Należy także zwrócić uwagę na to, że liczba fotonów, biorących udział w symulacji dla zwiększającego się kąta padania światła, nie może być stała, a także powinna rosnąć.

Porównano także multispektralne obrazy prawdziwej endogennej protoporfiryny IX i zasymulowanej zwykłej protoporfiryny, której macierz fluorescencji EEM była znana. Okazało się, że intensywności fotouczulacza na odpowiadających sobie zdjęciach są podobne, pomimo braku możliwości wygenerowania obrazów dla endogennej protoporfiryny IX – (rys. 6 i 7).

Wykonane obserwacje pokazują, że proponowany model oparty na metodzie Monte Carlo i mapach fotonowych daje wyniki zbliżone do rzeczywistych i może być używany do dalszych badań.

Address

Andrzej ZACHER: Politechnika Śląska, Instytut Informatyki, ul. Akademicka 16,
44-100 Gliwice, Polska, andrzej.zacher@polsl.pl .